

We thank the referees for the comments, which allowed us to improve the manuscript substantially. The following final authors response is repeating the interactive comment, where R#1 denotes Referee G. Chambon and R#2 stands for comments given by the second referee. We then provide our comment indicated as AC, followed by the new text inserted into the manuscript. We skip cases where we just took over the suggestions given, for better readability.

#### R#1: Overall comments

*R#1: The choice of the case studies appears a bit questionable, since none of them really challenges the 3D character of the model. A case of impact against an obstacle would have probably been better suited for that purpose.*

AC: The scope of the MS is to illustrate the potential of the 3-D model for cases that are typically addressed with depth-averaged approaches. In the case of impact against obstacles, we recommend to include the physics of the coarser colliding grains, which is part of the solver extension presented at EGU 2017. We will address impacts to obstacles in a separate work. It is difficult to find well-documented test cases with detailed measurements for the presented solver, so we limited the range of possible test cases to setups where all details were available to us.

*R#1: A more thorough discussion of the respective roles played by the slurry and granular contributions would have been interesting.*

AC: We agree, and we see the need for testing the simulation model with further experiments under the viewpoint of distinguishing the roles played by the granular and viscous rheology. However, as both the slurry and the granular rheology model include shear-thinning effects, it is difficult to come up with cases that show the contributions of each rheology separately and still illustrate the model applicability for real-world problems within one paper. However, we tried to address the role played by the granular rheology: we modeled an experiment of the USGS flume with enhanced roughness on the channel bed and compared the simulations of two different granular rheology parameters to illustrate the influence of the granular rheology on basal pressure, flow depth and front flow velocity. We then showed how the model performs in case of a granular dominated mixture with low slurry content, but on a smooth channel bed, which limits the influence of the pressure. To follow the given suggestions, we included a new discussion part addressing the influence of the pressure on the model (see the inserted text within the detailed comments section):

#### **“4.5: Contribution of the Coulomb-viscoplastic gravel representation within the flow process”**

The Herschel-Bulkley representation of the fine material suspension and the representation of the coarser grains as a Coulomb-viscoplastic fluid both introduce shear-thinning behavior to the flow process. An important role of the modeled gravel is the local viscosity increase as a consequence to a local pressure increase. Local pressure variations, as they may occur for example due to roughness elements, lead to a corresponding viscosity variation in the presence of modeled gravel, which in turn leads to a footprint of the pressure in the shear-rate distribution of the flow field, affecting both the slurry and the gravel rheology. Another consequence of the pressure-dependent rheology model of the gravel is the increase of the viscosity near the bed with increasing flow depth, which enhances the formation of steep flow fronts in the model. Consequently, the front flow depth development within the first half second of laser measurement is well captured in the large scale experiment (see last figure in the manuscript, however, the diagram at (b) lacks grain-size sorting effects). The pressure contribution affects the dam-break release, and one may recognize in Fig. 1 given below that the model is capable of representing the process. Although the front is steeper and arrives earlier due to neglecting the gate, the modeled maximum flow depth reaches the magnitude of the experiments, indicating a realistic material mobilization at least within the first two seconds.

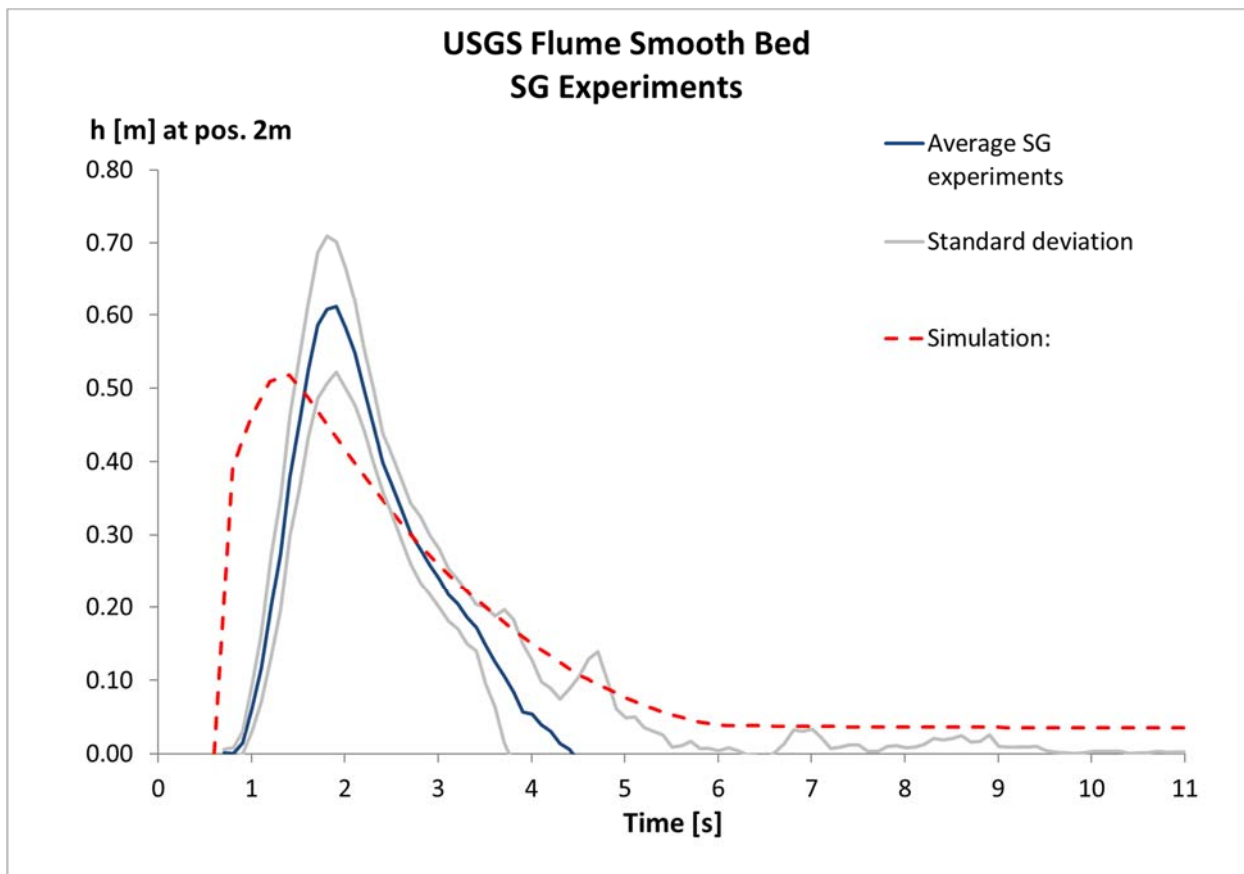


Fig. 1: Flow depth over time of the sand-gravel mixture 2 m below the release gate.

R#1: Detailed comments

R#1: *I would personally consider sand as belonging to the granular phase. However, as the authors systematically refer to this granular phase as “gravel”, one is led to think that sand is instead accounted for in the slurry. This issue would need to be better explained and discussed.*

AC: Sand-clay suspensions with water have been successfully modeled as shear-thinning viscoplastic materials by several authors in the past. Especially, O’Brian (1988)<sup>1</sup> derived from experiments “...that with increasing sand concentration, the viscosity remains comparable to that given from the clay content alone until the sand concentration exceeds about 20% by volume.” Sosio et al. (2009)<sup>2</sup> found that “The addition of sand finer than 0.106 mm has a negligible effect on it [viscosity] [...] Suspensions with up to 10% of sand have viscosities slightly higher than those composed of the fine fraction alone [...] The relationship between viscosity and total solid concentration deviates from the exponential dependency for sand particles larger than 0.300 mm and sand percentages larger than 35%.” Our Herschel-Bulkley rheology model for the slurry is parameterized on the basis of Yu et al. (2013)<sup>3</sup> where the material compositions were composed of clay minerals, fine sand, coarse sand, and a small amount (less than 5%) of gravel having diameters less than 10 mm. Yu et al. (2013)<sup>3</sup> introduced discontinuities in their modeled yield stress in dependency to the volumetric solid concentration and clay concentration. We added the following statement to the manuscript:

**“To be in agreement with the experiments of Yu et al. (2013)<sup>3</sup>, we consider all particles below 2 mm grain size as part of the interstitial slurry.”**

R#1: *It would be interesting to fully explicit the computation of the lumped rheology in at least some of the examples treated: i.e., give values of the “full” yield stress of the slurry  $\tau_{a\_y}$  (and not only of  $\tau_{a\_00}$ ); give values of the effective viscosities of the slurry and granular phases, and of the lumped material (concentration average), for representative shear rates and pressures. More generally, a discussion on the*

*interest of considering this composite constitutive law in the examples shown would be interesting. Is the contribution of the granular phase significant? Would have it been possible to obtain equivalent results with only the viscoplastic part?*

AC: We now address the suggested topic in the new discussion part addressing the influence of the pressure on the model.

#### **“3.4: Contribution of the Coulomb-viscoplastic gravel representation within the flow process**

The approach of a bulk-averaged viscosity derived from a Herschel-Bulkley representation of the fine material suspension and a Coulomb-viscoplastic representation of the gravel is based on the main assumption that the interstitial fluid can damp the grain collisions up to a degree where the tangential friction between gravel grains dominates the dissipation of the gravel phase. As an example at the limit of applicability, we have chosen a USGS flume experiment that applied a sand-gravel water mixture, in which the collision forces in general cannot be neglected. However, the selected experiment was conducted on a smooth channel bed, such that grain collisions were less pronounced and the video documentation shows a relatively dense material front where the grains are embedded in a slurry within the front. The experiment from the 21st of April 1994 is documented in Major (1997) with a release volume of  $9.2 \text{ m}^3$ , a dry bulk density at release between  $1630$  and  $1960 \text{ kg/m}^3$  and a maximal runout length of  $16.7 \text{ m}$ . For the flow process in the channel, ensemble-averaged data for 11 such smooth-channel SG mixture experiments is available (Iverson et al., 2010). The average wet bulk density at release is  $2070 \text{ kg / m}^3$  and the water volume within the release body averages  $3.17 \text{ m}^3$  for the smooth-channel SG experiments (Iverson et al., 2010). We simulate the experiment by representing the sand suspension with the Herschel-Bulkley rheology with 16% water content according to the average numbers for the SG smooth bed experiments (Iverson et al., 2010, table 2 and 3). The gravel is covered by the Coulomb-viscoplastic rheology. We used the same simulation grid as for the SGM smooth bed simulation and applied the same  $\tau_{00}$  value. The resulting Herschel-Bulkley rheology for the sand suspension had a density-normalized yield stress of  $\tau_y = 0.0526 \text{ m}^2/\text{s}^2$  and a corresponding consistency factor of  $k = 0.0158 \text{ m}^2/\text{s}^2.34$ . The Herschel-Bulkley exponent was chosen as  $n = 0.34$ . The volumetric share of sand suspension in the mixture was 57.5% and the gravel covers 42.5%. From the integration of the Herschel-Bulkley viscosity over the material volume at the moment of front arrival at the laser at position  $32 \text{ m}$ , we obtained a volume-averaged slurry viscosity of  $14 \text{ Pa s}$  that contributes with 57.5% to the overall viscosity. The corresponding volume-averaged gravel viscosity was  $54 \text{ Pa s}$ , contributing 42.5% to the overall viscosity. The modeled volume-averaged flow process 3.6 seconds after release was thus clearly dominated by the Coulomb-viscoplastic rheology. In a second step, we removed approximately half of the simulated material at  $3.6 \text{ s}$  after release by excluding cells with pressures over  $1500 \text{ Pa}$ , which led to a volume-averaged slurry viscosity of  $21 \text{ Pa s}$  and a Coulomb-viscoplastic average viscosity of  $49 \text{ Pa s}$ . Thus, the modeled material mixture was dominated by the gravel rheology even within the 50% of material that moved under lower pressures than the rest of the material. An adequate simulation of the experiment as achieved here (Fig. 12 e, f) is not possible only using a Herschel-Bulkley rheology with the parameters linked to the material as in (von Boetticher et al., 2016)”

R#1: *I did not really understand the rationale behind equation (1) used to evolve the parameter  $\tau_{00}$  with water content. In principle, one would expect this parameter to remain constant for a given composition of the solid material, and thus independent of water content. If I understood well, the authors do nevertheless consider a variation of  $\tau_{00}$  with water content due to a sensitivity of their computations, in particular shear rate, to grid size. From my point of view, this issue should be discussed in more details (see also comment 4 below), and equation (1) should be better justified. In some sense, it can seem disappointing to develop a full 3D model relying on supposedly physically-based constitutive models and, in the end, to use such a trick to resolve what seems to be a purely numerical issue. In particular, the grid-size-sensitivity probably implies that the vertical structure of the flow is relatively poorly captured in the presented simulations. What is then the benefit of the 3D model compared to a depth-averaged approach?*

AC: As pointed out in the companion paper, “When simulating laboratory flume experiments where debris-flow material accelerated in a relatively narrow and short channel (Scheidl et al., 2013), a cell height of 1.5 mm, which is of the order of the laboratory rheometer gap, was still not fine enough to reach the limit of grid sensitivity.” The grid-size-sensitivity is mainly a consequence of thin layers of high shear as they may appear in debris flows and is less dependent on the overall vertical structure of the flow. However, the correct location, extent and temporal variation of such shear bands is one of the benefits a 3D model can provide compared to a depth-averaged approach. The Herschel-Bulkley rheology of the slurry provides the shear stress as the sum of a shear-rate dependent term and a yield stress. The yield stress is estimated based on material composition due to Yu et al. (2013)<sup>3</sup> and the shear-rate dependent term is a linear function of the yield stress. However, the shear-rate dependent term is a non-linear function of the shear-rate and thus sensitive to the grid discretization *and* the flow characteristics. Our calibration parameter  $\tau_{00}$  is not precisely adequate to a physically based parameter because it embodies a countermeasure for grid resolution issues. Although it is multiplied with the function of the volumetric concentrations of clay  $P_0$  and solids  $C_v$  defined in Yu et al. (2013)<sup>3</sup> to form the Herschel-Bulkley yield stress, the adjustment of  $\tau_{00}$  should as well overcome the overall disagreement between modeled and real shear stresses for a given calibration case and grid resolution. Even a model that would perfectly adapt to a change in material composition would still face the problem that the change in viscosity due to the new material composition affects the shear rate of the flow which in turn leads to a grid resolution sensitive amplification of the change in shear stress. In a first step, we thus enhance the modeled effect of material composition changes by applying the same relative change to the model parameter.

Please note that the transfer of  $\tau_{00}$  with equation 1 for the simulation of the 30% water content experiment in the previous manuscript was inconsistent with the other experiments by applying a clay concentration  $P_0$  by mass, not by volume. The published model uses the volumetric clay content  $P_0$  as suggested by Yu et al. (2013) and we updated the simulation in the current manuscript accordingly. The corresponding adjustment of the model to changed water contents is still underestimating the water content sensitivity and we see that further research is necessary to find improved modifications of  $\tau_{00}$  in dependency to changes of the material composition.

R#1: *Nothing is said concerning the mesh characteristics used in the different examples presented: grid size, number of elements in the horizontal and vertical directions, etc.*

AC: We altered the manuscript and now provide the number of cells in horizontal and vertical directions:

### **“3.2 Grid resolutions**

**In general, we distinguished between channelized flows and flows on a plane in choosing our grid resolutions. We first defined a necessary resolution in the flow direction and transverse to the flow to capture the channel geometry. In case of channel flows, we then considered the surface velocity gradients at characteristic front flow velocities in the flow direction and transverse to the flow direction. We kept the ratio between cell length and cell width smaller than the ratio between these longitudinal and transversal velocity gradients and smaller than ten. In case of flows on a runout plane, we kept the ratio below 2.5. The vertical grid resolution was then defined by the available computational resources in a way that results were obtained within reasonable time. The mesh size used for the water content sensitivity experiments increased from 1 mm cell height at the bottom to 4 mm cell height at a distance 25 mm above the bed. This height of 25 mm corresponds to the maximal surface elevation reached at the position of the laser measurement situated one meter downslope of the gate. The cell width was constant 1 cm and the cell length was 2.3 cm.**

The curved channel experiment was modeled with 39 cells in radial direction and a radial grading from 1 mm cell height and 2 mm cell width at the bed to 3 mm cell height and 2 mm cell width 6.5 cm above the bed. In flow direction, the resolution was constant with a cell length of 5 mm. The USGS flume with a smooth channel bed had approximately 4 million cells to model the channel flow, which led to a constant cell length of 28 cm, a cell width of 3.3 cm and a grading cell height from 0.7 cm at the bottom to about 1 cm cell height at 19 cm above the bed, which is the highest point reached by the free surface at the laser 32 m downslope of the gate. The runout was modeled with 10 million cells with the same vertical resolution and 5 cm cell sizes in x and y directions. The USGS flume with bumps was represented with 6.5 million cells on a refined mesh, resulting in 1.5 cm cell length, 1.25 cm cell width and 1.4 cm cell height at the bottom. Three cell layers above the bottom the mesh coarsened in lateral and bed-normal direction to 4.4 cm cell length and 2.1 cm cell height. At a height of 32 cm normal to the bed, the mesh coarsened again in the horizontal direction and was continuously graded vertically; however, the corresponding cells were in the air phase of the flow except for the release body. During release, the upper part of the material lies within the coarse mesh, but during column collapse as the flow accelerates, this material transits into the finer mesh closer to the bed, where it starts shearing. We performed a grid resolution sensitivity analysis with the modeled experiments of the water content sensitivity study, as described below.”

*R#1: The influence of grid size on the presented comparisons with experimental results would also need to be discussed, in particular, whether the results presented in Fig. 5 for the reduced and increased water contents (compared to the calibration case) could be improved with a finer mesh. Same question for the results presented in Fig. 15, notably the strong unphysical oscillations displayed by the pressure signal.*

AC: The grid resolution of the USGS flume needed to be fine enough to capture the basal roughness, and we had to simplify the shape of the bumps on the bed because we reached the limit of applicability due to high computational times, which makes the setup unsuitable for grid resolution studies. We see the strong pressure oscillations in Fig. 15 as a consequence to the simplified shape of the basal roughness elements (pyramids instead of cones). We carried out a grid sensitivity analysis for the experiments shown in Fig. 5 and included the findings in the altered manuscript, corrected a mistake in the composition of the 30% water content experiment simulation (see previous section) and changed the displayed deposits in Fig.5. (In the original MS we showed the wetted slope of the simulations as deposit shape, now we show the material surface defined as the region with a modeled air concentration of 0.5):

**“We simulated the three different water content experiments using a coarser grid resolution with twice the cell length, width and height, and conducted the same simulations on a finer mesh that reduced the cell width, length and height by one third. The reduced numerical costs of the coarser mesh allowed running the simulations once without recalibration and once with a recalibration of the experiment with 28.5% water content to the new coarse mesh, followed by adjusted coarse-mesh simulations of the 27% and 30% water content experiments using equation (1).**

**We did not perform a recalibration with the refined mesh due to numerical costs. We only simulated the experiments on the finer mesh applying the original calibration parameter. Table 1 lists a comparison of the resulting runout distances.**

**Table 1: Comparison of modeled and measured runout distance  $L$  for different mesh resolutions and water contents**

| Water content | L coarse mesh        | L coarse mesh recalibrated | L fine mesh  | L measured |
|---------------|----------------------|----------------------------|--------------|------------|
| 27 %          | 2.47 m               | 2.36 m                     | 2.25 m       | 2.00 m     |
| 28.5 %        | 3.41 m               | 3.23 m                     | 3.05 m       | 3.20 m     |
| 30 %          | 4.61 m               | 4.31 m                     | 4.32 m       | 4.83 m     |
| Water content | Deviation abs., rel. |                            |              |            |
| 27 %          | 0.47 m, 47%          | 0.36 m, 18%                | 0.25 m, 13%  |            |
| 28.5 %        | 0.21 m, 7%           | 0.03 m, 1%                 | -0.15 m, -5% |            |
| 30 %          | -0.22 m, 5%          | -0.52 m, 11%               | -0.51 m, 10% |            |

Recalibrating the 28.5% water content experiment to the coarse mesh, we changed  $\tau_{00}$  from 41.3 Pa to 45.0 Pa to achieve 1% precision in runout prediction. We repeated the adaptation of  $\tau_{00}$  to the water content of 27% and 30% using equation (1), which led to a change of  $\tau_{00}$  from 33.5 Pa to 36.5 Pa for the 30% water content mixture and to  $\tau_{00} = 56.3$  Pa instead of 51.8 Pa in case of the 27% water content mixture. We address other aspects of the grid sensitivity in the discussion section.”

AC: In the discussion we further address the grid sensitivity study:

“The discrepancy in runout length of the water content sensitivity tests could not be reduced with better grid resolutions for all the three water contents because the model showed a general trend to decrease the runout distance with increasing grid resolution. The mesh resolution study showed a consistent decrease in runout distance with increasing grid resolution. The modeled experiment with 28.5 % water content on the finer mesh underestimated the runout distance by 15 cm or 5% whereas the coarse mesh without recalibration increased the runout prediction by 21 cm or 7%. The relative decrease in maximal runout due to the increased grid resolution, defined as  $(\text{runout coarse mesh} - \text{fine mesh}) / (\text{average between runout coarse mesh and fine mesh})$ , was 9% for the lower water content mixture, 11% in case of the calibration experiment and 7% for the increased water content simulations. The enhanced underestimation of the runout with 30% water content due to a fine grid resolution counterbalanced the slight improvement obtained on a finer grid in the reduced water content experiment.

In the reduced water content experiment, the mobilization of the release body was slower than in the experiments with higher water contents. In the 27% water content experiment, the front arrival time at the laser decreased with increasing grid resolution from about 0.6 s after release for the coarse mesh, to 0.8 s in case of the original mesh, and 1.2 s in the fine grid simulation. For this experiment, we integrated the modeled downslope velocity over the material volume close to the moment of front arrival at the laser. By dividing the volume-integrated velocity by the debris volume at this time step, we obtained a volume-averaged downstream velocity of about 1.3 m/s in case of the coarse grid and 1.1 m/s for the fine grid at the moment of front arrival at the laser. The corresponding volume-averaged slurry and gravel viscosities were 4.8 Pa s and 7.2 Pa s for the coarse mesh and 13.9 Pa s and 9.3 Pa s in case of the fine mesh.

The pronounced difference between the two mesh resolutions, especially with respect to the volume-averaged Herschel-Bulkley viscosity, indicate higher shear rates on coarser meshes during release, which lead to faster flows due to the non-linear rheology. The recalibrated coarse mesh simulations indicate that the free model parameter can counteract the consequences of changing shear rates that are caused by altered mesh resolutions.

On the fine mesh, front fingering occurred before the material came to rest, which only appeared when using a Coulomb-viscoplastic rheology together with the volume-of-fluid method. The volume-of-fluid method, in general, tends to split the material into droplets when the flow depth

becomes small. This effect remains even in hybrid approaches like the coupled level set-VoF method [Wang et al. 2008<sup>4</sup>]. The debrisInterMixing solver thus tends to develop splashes that separate from the main material body in case of shallow runout deposits. A multiphase model that solves one Navier-Stokes equation for each phase or a coupled Lagrangian particles simulation are needed to treat the development of the granular flow front accurately, but this would severely increase the computational costs.”

1: O'Brian: *Laboratory analysis of mudflow properties*, Journal of Hydraulic Engineering, Vol. 114, No 8, 1988.

2: R. Sosio, G. B. Crosta: *Rheology of concentrated granular suspensions and possible implications for debris flow modeling*, Water Resources Research, DOI: 10.1029/2008WR00692, 2009.

3: Yu, B., Ma, Y., and Qi, X.: *Experimental Study on the Influence of Clay Minerals on the Yield Stress of Debris Flows*, J. Hydraul. Eng., 139, 364–373, 2013.

4: Z. Wang, J. Yang, and F. Stern: *Comparison of Particle Level Set and CLSVOF Methods for Interfacial Flows*, 46th AIAA Aerospace Sciences Meeting and Exhibit, Aerospace Sciences Meetings, DOI: 10.2514/6.2008-530, 2008

#### Technical comments by R#1:

In general, we changed the manuscript according to the reviewer suggestions. In the following we comment on changes that demand explanation. Comments include the page number P. and line number l. of the original manuscript.

R#1: P.3, l. 25: “Therefore, for each material composition there should be a critical range where a minor variation in water content causes a strong change in flow depths and run-out distance.” I do not really understand this statement. How is this “critical range” related to the exponential variation of the yield stress with water content?

AC: We changed the text to: “**Therefore, a minor variation in water content may cause a strong change in flow depths and run-out distance**” removing the statement about a range that has a specific high water content sensitivity, because such a range is defined by many factors.

R#1: P.6, l.11-12. Please also indicate the experimental values of  $\tan(\beta_{\min})$  and of the corresponding correction factor.

AC: We changed the text to “...which fits the experimental average of  $\tan(\beta) = 0.33 \pm 0.05$  (Scheidl et al. (2015) table 2) and the corresponding correction factor  $k^* = 2.1 \pm 0.6$ .” The experimental  $\tan(\beta)$  is given as a best fit straight line derived from the three laser measurement points and we do not have the resources to construct the set of experimental values  $\tan(\beta_{\min})$  for all tests. Looking at a representative experiment “Test A 6040\_2” shows that the inner Laser No 1 does not register any material at the time of the maximum surface super elevation (Fig. 2 below), and a corresponding experimental  $\tan(\beta_{\min})$  would be 0.37.

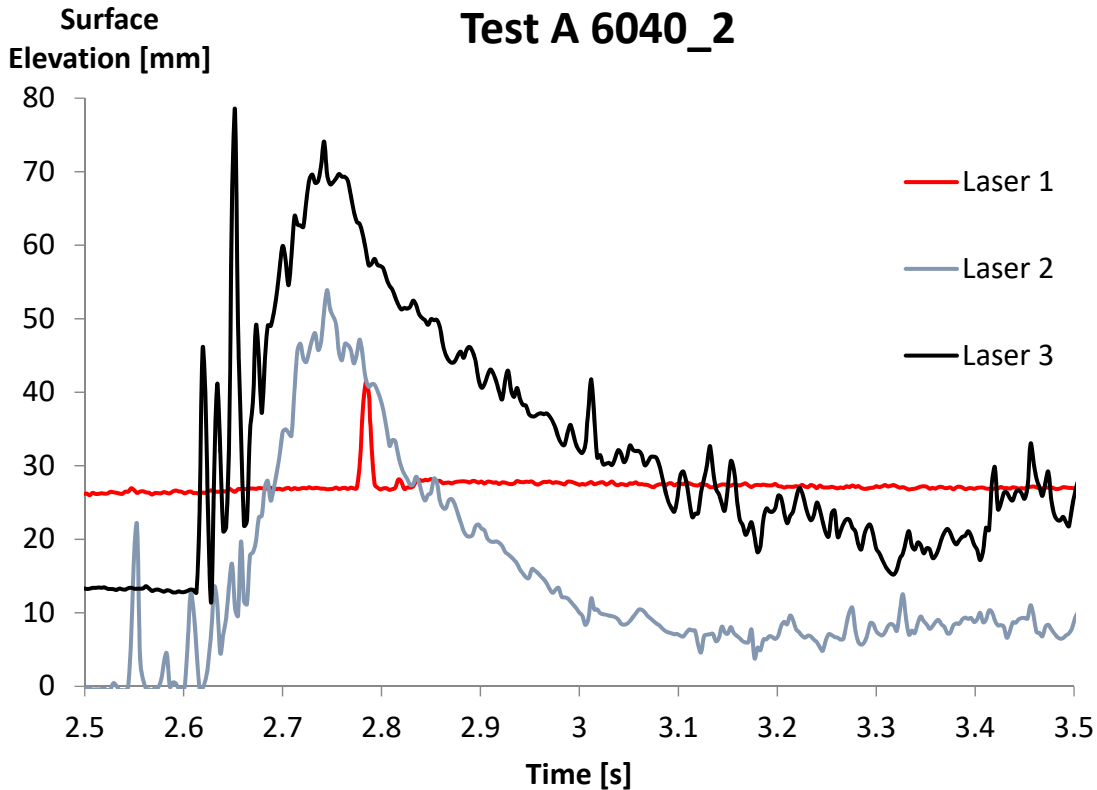


Fig. 2: Example of measured laser time series in a curved channel experiment with 20° slope inclination and mixture A.

R#1: P.7, I.5-7. Why were simulations of the SG mixture based on the same calibration parameters as for the SGM mixture? Since the composition of these two materials is different, it seems that a recalibration would be necessary? Furthermore, results obtained with SG mixture are not really described in the following (and Fig. 8 is never properly discussed). What is then the point of introducing this additional case?

AC: The case is introduced to show an application of the model where the composition does not contain enough fine material to damp granular collisions, but the absence of channel roughness seems to allow a viscoplastic approach to model the flow. We now use this additional case as main contribution to illustrate the role of the Coulomb-viscoplastic gravel representation in the newly introduced section. The calibration for the smooth channel bed was done for the SGM experiment introduced in the previous section, based on the front arrival of the corresponding test of 26<sup>st</sup> of May 1994 published in Major (1997), and as the simulation grid does not change, the model can approximately adjust to the new mixture without recalibration. However, we changed from  $\tau_{00} = 82.78$  which was by mistake taken over from the SGM simulation on the rough channel to  $\tau_{00} = 90$  as in the smooth channel SGM simulation.

R#1: P.10, I.21-23: "The measured and simulated values do not agree with the mean arrival times implied by the laser signal at position 66 m (Fig. 15 b), however, they do by means of basal pressures for the lower gravel friction angle simulation (Fig. 15 d)." Unclear sentence.

AC: We reformulated the sentence accordingly: "The measured and simulated values do not agree in terms of the mean arrival times implied by the laser signal at position 66 m (Fig. 12 b) however, when we use the basal pressure signal as an indicator of the front arrival, the measured and simulated arrival times fit well in case of the lower gravel friction angle simulation (Fig. 12 d)."



R#1: P.11, l.1. I do not fully understand what the authors mean by “Our approach allows the model parameters to be linked to (. . .) local topography”.

AC: We made the statement more clear: **“Our approach allows the model parameters to be linked to material properties and the model accounts for effects of the local topography on the shear stresses within the material.”**

R#1: P.12, l.1: “The model can account for the sensitivity of the rheology to channel geometry . . .”. This is a strange statement: one does not expect the rheology (a material property) to be sensitive to channel geometry.

AC: We now state: **“The model can account for the pressure and shear-rate dependent viscous stresses and thereby captures the sensitivity of the material behavior to channel geometry.”**

R#1: P.12, l.8-10: “Because such changes in model setup are translated into consequences for the flow physics by the model, the ensemble of such simulations may mirror how the modeled site would respond to similar changes.” Unclear sentence.

AC: We try to make the statement more clear: **“Because such changes in model setup are translated into consequences for the flow physics by the model, the ensemble of such simulations could be used to outline the consequences of changes at the site. For example, a change in topography by a construction, a change in expected water content by a drainage or a change in expected debris flow compositions by a new gravel deposit could be addressed with the model to visualize the corresponding changes in expected debris flows.”**

Comments on figures: We followed the given suggestions.

The following comments by referee #2 include the page and line numbers of the original MS, the comments refer to.

R#2: Overall comments

R#2: As the present MS is the application of Part I, the Introduction/Discussion should briefly mention the need of the full 3D simulations, modeling assumptions, simplicity for application as well as the scopes/limitations of the modeling and simulation approaches as mentioned in Part I. This would help the audience who may only focus on application, to directly follow this paper

AC: We added a statement in the introduction pointing out the potential of 3D simulations in comparison to depth-averaged approaches:

**“In contrast to the common depth-averaged model approaches for debris flow simulation, this model resolves the flow process in three dimensions. Thus the strong coupling between the flow behavior and the channel geometry and basal roughness can be addressed as shown within this work.”**

AC: The revised manuscript has a first section where we briefly summarize key assumptions and the approach of the model as well as its restriction to high contents of fine material:

**“The model, as described by von Boetticher et al. (2016), is based on an adaptation of the interMixingFoam solver of the open source finite volume code OpenFOAM. We linked the Herschel-Bulkley rheology parameters to the composition of the material mixture and assumed that high contents of fine material such as the interstitial suspension between the gravel grains can**

damp grain-to-grain collisions Under this assumption, the gravel can be treated as a Coulomb-viscoplastic fluid with the pressure-dependent rheology model of Domnik et al. (2013). The stable implementation together with the reduction to two free model parameters allows reliable numerical studies of three-dimensional flow processes of debris flows that have high shares of fine material. The bulk mixture is combined with an air phase by the Volume-of-Fluid method (Hirt 1981) to capture the free surface In addition to determining typical material parameters (density, water content and relative amounts of gravel and clay), the user is required to input the clay composition (e.g., the fractions of kaolinite and chlorite, illite, montmorillonite; (Yu et al. 2013), and  $\delta$ , the friction angle of the gravel fraction, approximated as its angle of repose. To be in agreement with the experiments of Yu et al. (2013), we consider all particles below 2 mm grain size as part of the interstitial slurry. The two remaining calibration parameters are related to the fine material suspension. One of the two free model parameters, the Herschel-Bulkley exponent  $n$ , was kept constant and set to 0.34, which was suitable for all simulations presented here. Due to that, the only parameter modified for calibration was  $\tau_{00}$ , which acts as a multiplication factor for the calculated yield stress of the fine sediment suspension. In case of dense mixtures where the volumetric solid concentration exceeds a threshold of 0.47, the model amplifies  $\tau_{00}$  as defined in Yu et al. (2013).”

R#2: *Writing could be substantially improved in concept and content.*

AC: The concept of the paper was to illustrate the model sensitivity to water content, channel geometry and channel bed roughness, and the content followed that concept by presenting the corresponding selected experiments and their simulation. We now make the concept more clear by stating:

**“The objective of this study is to illustrate the model's ability to accurately account for a wide range of flow behaviors without recalibration. The key attributes of the model are its sensitivity to water content, gravel- and clay-fraction and clay-mineralogy on the one hand (also see de Haas (2015)), and the interaction between the phase-averaged bulk rheology of the mixture and the complex three-dimensional flow structure on the other.**

**We first present validation test cases that focus on water content sensitivity in laboratory scale, followed by a model setup to analyze the effect of enhanced free surface elevations due to channel curvature. We then study the model's capability to adapt to basal roughness using large-scale flume experiments. Finally, we illustrate the role of the gravel rheology on the overall simulation results using large-scale experiments with a water-sand-gravel mixture. We discuss limitations of the model set-up based on these simulation results.”**

R#2: *Some important dynamical aspects observed in the simulations would have been explained in a better way with elaboration.*

AC: In accordance with the comments given by reviewer #1, we now present the role of the coulomb-viscoplastic rheology in an own section (see Authors comment to reviewer #1).

R#2: *In a debris flow body, water content may evolve strongly (Pudasaini and Fischer, 2016; Mergili et al., 2017), and the characteristic may range from dense to dilute flows. These aspects need to be clearly mentioned in the MS. Recent and relevant literatures could be included and discussed.*

AC: We agree and included the suggested literature.

R#2: Detailed comments

AC: We agree with most of the comments and only list here the changes that went beyond the suggested improvements or explain why we did not follow the suggestions.

R#2: *Abs.: material properties were known → material properties and compositions were known*

AC: As we list the compositions within the following enumeration, we think it is clear that the composition is seen a property of the debris flow mixture.

R#2: *(including its mineral composition): Remove*

AC: The presented work is the first debris flow model that accounts for the clay mineral composition, therefore we should mention this within the abstract. The necessary model ingredients are now mentioned as:

**“For the selected experiments in this study, all necessary material properties were known -- the content of sand, clay (including its mineral composition) and gravel as well as the water content and an angle of repose of the gravel. Given these properties together with the density of the mixture, two model parameters are sufficient for calibration, and a range of experiments with different material compositions can be reproduced by the model without recalibration.”**

R#2: *two model parameters are sufficient for calibration → two model parameters are used for calibration*

AC: We cannot change the statement that way because we use only one parameter for calibration, however, from previous discussions we know we should mention that two parameters are available for calibration.

R#2: *The angle of repose: is this ‘the angle of repose’ of ‘internal friction angle’?*

AC: The internal friction angle is difficult to measure for coarse gravel, whereas it is simple to estimate an angle of repose from the material deposits in the field. Whenever available, we used the angle of repose as a measure for the granular friction. However, we used the internal friction angle as an alternative approximation in the large scale experiments.

R#2: *P2: L24: a restricted multiplication factor: Explain.*

AC: We changed the statement to:

**“Due to that, the only parameter modified for calibration was  $\tau_{00}$ , which acts as a multiplication factor for the calculated yield stress of the fine sediment suspension. In case of dense mixtures where the volumetric solid concentration exceeds a threshold of 0.47, the model amplifies  $\tau_{00}$  as defined in (Yu et al. 2013).”**

R#2: *L33: We mention that super-elevation has been analytically modeled and validated for dry granular flows and flows of mixtures by Pudasaini et al. (2005, NHESS; 2008, PoF)*

AC: We added the reference to the literature, but instead of summarizing the general discussion content we point out a difference to this study by naming its depth-averaged approach:

**“We mention that effects of curvature were analytically modeled and validated for dry granular flows and flows of mixtures by (Pudasaini et al. 2005, Pudasaini et al. 2008) with a depth-averaged approach.”**

R#2: P3: L21: *Since, in the mixture, largely the solid particles exhibit slip, viscous fluid exhibits no-slip along the basal surface such distinct basal boundary conditions can only be included with real two-phase mass flow models (see, e.g., Pudasaini, 2012; Mergili et al., 2017).*

AC: We included the statement as:

**“In general, largely the solid particles exhibit slip and viscous fluid exhibits no-slip along the basal surface. Only through the core assumption of identical velocity between gravel and surrounding fluid due to high drag do such distinct basal boundary conditions reduce to a no-slip condition. OpenFOAM offers partial-slip boundary conditions, however, the definition would only become meaningful together with real two-phase mass flow models as in Pudasaini (2012); Mergili et al., (2017), or as developed by Wardle (2013) within our 3D framework.”**

R#2: P4: *The mixture effectively consists of water, fine particles and gravel with different physical parameters and mechanical, hydrodynamical response to applied loads. In such a complex situation, how a simplified model with two free parameters can capture the flow so nicely. It needs to be discussed. There is an almost perfect fit between the shapes of the experimental and simulated deposits in the calibration case (Figure 5 center).: Explain the reliability of the perfectness, because the other two panels do not so strongly support this statement.*

AC: As can be seen from the comparison of the modeled flow depth with laser data, the depth of the flow along the material body is well captured by the model in general. As we calibrate the model to fit the maximal runout and thus capture the longitudinal profile is well, the overall width of the deposit matches the experiment more-or less as a consequence of volume conservation. The local width of the deposit is adjusting the transversal surface gradient to balance the hydrostatic pressure at the center line. Again, as the hydrostatic pressure along the center line is well captured, the width of the deposit performs well, too. However, we had an inconsistent application of the share of clay in terms of mass and in terms of volume in case of the 30% water content experiment, and the model adjustment to water content changes is now less exact but more consistent (the sensitivity is underestimated for both decreasing and increasing water contents). But by adjusting  $\tau_{00}$ , an adequate fit can be achieved for other water contents, too: Fig. 3 shows the final deposit for the 30% water content experiment with  $\tau_{00}$  recalibrated to 24 Pa.

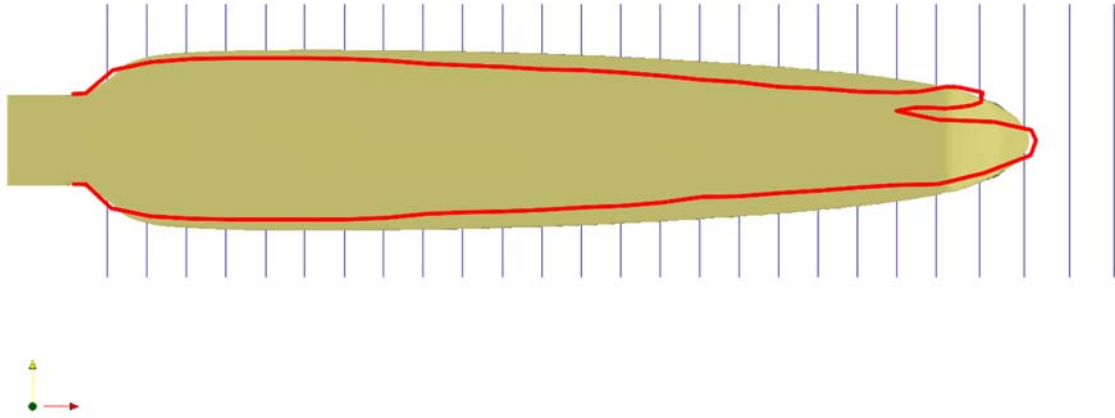


Fig. 3: Measured deposit (red line) and simulation of the 30% water content experiment after recalibrating the free model parameter to 24 Pa match the maximal runout.

R#2: L6-11: *Improve.*

AC: We simplified the text to be more clear:

**“An initial and simple approach chosen here is to first evaluate the relative effect that a changed water content has on the modeled Herschel-Bulkley yield stress  $\tau_y$ . In a second step, we apply the same relative change to the calibration parameter  $\tau_{00}$ . Let  $\tau_{newycal}$  be the Herschel-Bulkley yield stress calculated by the model for a new water content, based on the original value of the calibration parameter  $\tau_{00cal}$  that is not yet adjusted to the new water content. We reduced or increased the free model parameter  $\tau_{00}$  according to equation 1, where  $\tau_{00cal}$  denotes the Herschel-Bulkley yield stress as calculated by the model in the calibration test before the water content changed.”**

R#2: *Even if the flow height is twice the maximum grain size what about the experimental simulation reliability/reproducibility/accuracy?*

AC: We added a grid sensitivity analysis section, as commented in the reply to reviewer #1. We repeated the simulation of the 28.5 water content on three different clusters in the ETH domain (Hera, Brutus, Euler) and on a Centos machine as well as on a Ubuntu laptop without noting any difference in results.

R#2: P5:

L1-2: *However, the simulated front also temporarily paused at  $x = 2.04$  m, until it was overrun by a second wave 0.1 s later: Not shown.*

AC: We removed that statement.

R#2: L3-4: *The maximum flow depth and the subsequent decrease are well reproduced (Figure 4 center): There is no flow depth here; in Fig. 4 hydrograph, in Fig. 5 only deposition areas are shown.*

L3-9: *There is a non-logical switching between Fig. 4 and Fig. 5; difficult to follow.*

AC: The figures show flow depth over time, not a hydrograph.

R#2: L12: *However, super elevation also occurs in dry granular flows as this phenomenon is primarily induced by the geometry of the channel (curvature and twist) rather than the viscous or frictional properties of the material.*

AC: We consider enhanced super elevation as highly dependent on frictional properties.

R#2: L12: *so it can be viewed as a further indicator for model quality. → so it can be viewed as a further indicator for model quality (from geometric point of view).*

AC: The enhanced surface elevation is the result of a flow process and has the same potential for quantitative comparison of models with experiments as front position over time or flow depth.

R#2: P6:

L6: *For this a mechanical phase-separation model (Pudasaini and Fischer, 2016) would be required.*

AC: We added:

**“To account for the granular flow front, a mechanical phase-separation model like that described by (Pudasaini and Fischer, 2016) would be required, or even a coupled Lagrangian particle simulation.”**

R#2: L14: *the front volume: not clear/not seen.*

L21-22: *Does it upscale?*

AC: We could not yet remodel the experiment to larger scales.

R#2: P7:

L18: *Separation between solid- and fluid-type materials may lead to this discrepancy that can be described with phase-separation model (see literature mentioned above).*

AC: Although the separation in a granular front and a viscous tail may be described with phase-separation models, the surges addressed here, to our understanding, originate from the reservoir. We tracked such surges in the video documentation from the reservoir down, in the three experiments as shown in Fig. 10 of the new manuscript. With a smooth channel bed as discussed at P7 L18 in the original MS, the corresponding grain size sorting is even less pronounced.

R#2: L15-16: *This discrepancy could have been emerged due to the fact that there could be substantial interactions and also separation between solid- and fluid-type phases that has not been considered in the simulations.*

AC: We tend to agree with Iverson (2010) and see the reason for different front arrival times between basal pressure and laser measurements in single grains jumping ahead that are only captured by the laser.

R#2: P9:

L7-8: *Only grid-resolution (numerical) is explained as a possible source of discrepancy. But this discrepancy could also be reduced by applying real two-phase models with explicit phase-interactions. Needs discussion.*

AC: We added a grid sensitivity analysis section to the text and rewrote the discussion of the water content sensitivity experiments accordingly:

**“The simulations of the small-scale experiments that focus on water content sensitivity could reproduce the pronounced dependency of the run-out length on water content with some underestimation of the effect. The model could predict flow depth developments over time. Some short-time peak deviations between observations and simulations reached values close to the maximum grain size, possibly resulting from single-grain effects. The underestimation of the influence of the higher water content led to a run-out under-prediction by 15% in the model compared to the observation. The deposit of the calibration test case was accurately reproduced by the model, but the run-out of the reduced water content experiment was over-predicted by 17%.**

The discrepancy in runout length of the water content sensitivity tests could not be reduced with better grid resolutions for all the three water contents because the model showed a general trend to decrease the runout distance with increasing grid resolution. The mesh resolution study showed a consistent decrease in runout distance with increasing grid resolution. The modeled experiment with 28.5% water content on the finer mesh underestimated the runout distance by 15 cm or 5% whereas the coarse mesh without recalibration increased the runout prediction by 21 cm or 7%. The relative decrease in maximal runout due to the increased grid resolution, defined as  $(\text{runout coarse mesh} - \text{fine mesh}) / (\text{average between runout coarse mesh and fine mesh})$ , was 9% for the lower water content mixture, 11% in case of the calibration experiment and 7% for the increased water content simulations. The enhanced underestimation of the runout with 30% water content due to a fine grid resolution counterbalanced the slight improvement obtained on a finer grid in the reduced water content experiment.

In the reduced water content experiment, the mobilization of the release body was slower than in the experiments with higher water contents. In the 27% water content experiment, the front arrival time at the laser decreased with increasing grid resolution from about 0.6 s after release for the coarse mesh, to 0.8 s in case of the original mesh, and 1.2 s in the fine grid simulation. For this experiment, we integrated the modeled downslope velocity over the material volume close to the moment of front arrival at the laser. By dividing the volume-integrated velocity by the debris volume at this time step, we obtained a volume-averaged downstream velocity of about 1.3 m/s in case of the coarse grid and 1.1 m/s for the fine grid at the moment of front arrival at the laser. The corresponding volume-averaged slurry and gravel viscosities were 4.8 Pa s and 7.2 Pa s for the coarse mesh and 13.9 Pa s and 9.3 Pa s in case of the fine mesh.

The pronounced difference between the two mesh resolutions, especially with respect to the volume-averaged Herschel-Bulkley viscosity, indicate higher shear rates on coarser meshes during release, which lead to faster flows due to the non-linear rheology. The recalibrated coarse mesh simulations indicate that the free model parameter can counteract the consequences of changing shear rates that are caused by altered mesh resolutions.

On the fine mesh, front fingering occurred before the material came to rest, which only appeared when using a Coulomb-viscoplastic rheology together with the volume-of-fluid method. The volume-of-fluid method, in general, tends to split the material into droplets when the flow depth becomes small. This effect remains even in hybrid approaches like the coupled level set-VoF method [Wang et al. 2008<sup>4</sup>]. The debrisInterMixing solver thus tends to develop splashes that separate from the main material body in case of shallow runout deposits. A multiphase model that solves one Navier-Stokes equation for each phase or a coupled Lagrangian particles simulation are needed to treat the development of the granular flow front accurately, but this would severely increase the computational costs”

R#2: L20: *As mentioned previously other relevant works could be discussed.*

L21: *Discuss the work by de Haas et al. (2015) and for grain sorting and phase separation that can be modeled by the phase-separation model mentioned above.*

AC: We had a long review of previous debris flow models in the first paper version and a discussion section of models with comparable approaches in the last paper version, but as a result of the open discussion of the previous articles, we focus on the abilities and drawbacks of this model presented here and do not discuss other model approaches, especially as the text is already long.

R#2: L26: *from the experiments. → from the experiments. This is clear because, to improve this it requires explicit inclusion of both the curvature and twist of the channel with full control over these geometric properties in the model equations (Pudasaini et al., 2005, 2008; Fischer et al., 2012) that has been included here implicitly through the three-dimensional flow simulations.*

R#2: We do not agree, as we consider the three dimensional finite volume or finite element approaches superior in accuracy to depth averaged approaches. The difference in volume originates from the simplified release box, were the original transition to a half-pipe channel caused the material to jump and include air bubbles, something that can be captured with appropriate high grid resolution but cannot be captured by the models mentioned by the reviewer.

R#2: L27: *by the no-slip boundary condition, → by the no-slip boundary condition, that could be improved by applying the automatically evolving pressure- and rate-dependent Coulomb-viscoplastic mechanical basal slip conditions developed by Domnik et al. (2013).*

AC: We added:

**“One could reduce the amount of material sticking to the walls by applying partial slip conditions like in Domnik et al. (2013), however, this would demand a multiphase approach to account for the wetting of the walls, which goes beyond the scope of this model.”**

R#2: P10:

L10-11: *I: Such discrepancy could be reduced with phase-separation model.*

L25: *Also discuss phase-separation effects that might dominate the flow dynamics.*

L29: *I: This clearly demands for two- or, multi-phase flow model with phase-separation mechanisms.*

AC: We now briefly mention the possible approaches to account for phase separation:

**“Phase separation effects would need to be taken into account by implementing either drift-flux models, multiphase approaches with one Navier-Stokes equation per phase or coupled Lagrangian particles or coupled discrete element methods. However, the corresponding model extension would introduce new model parameters and higher numerical costs. As a consequence of our reduced approach without grainsize sorting effects, we did not model the run-out patterns of the rough channel experiments, in contrast to the smooth channel experiment where less demixing occurred.”**

R#2: P11: L6-11: *The new model overcomes a weak point of debris flow modeling: These statements are not fully valid. This discussion should be compatible with Part I. It would be better not to state ‘overcomes a weak point’ but in practical applications ‘just reduces the complexities’. Drag is an essential component of mixture flows. To simplify the situation, and also depending on the flow type, it could be considered to be negligible.*

*Except in local regions, globally flows are essentially thin that can be very economically simulated with real two-phase models that also includes drag (Mergili et al., 2017). So, such descriptions on drag do not help so much in the MS.*

L10: *difficult to quantify → difficult to quantify. However, Pudasaini (2012) developed a generalized drag model that overcomes these difficulties. Real complex flows cannot*



*always be modeled by just applying largely oversimplified models. These are different modeling approaches.*

AC: We now name it “**reduces the complexities**” instead of “overcomes a weak point”. The corresponding section is inspired by the feedback of applicants in the debris flow protection domain and is in fact the main motivation for the presented work.

R#2: L12-14: *Not fully true, see other works mentioned above.*

AC: As long as there is no published work modeling such variety of flows, mixtures and scales with one parameter, we consider our statement as true.

Comments on figures: We followed the given suggestions where possible, exceptions are discussed below.

R#2: *Fig. 13: Remove*

AC: The figure explains the inhomogeneous time development of the flow front positions in the previous figure, which is the core figure of the paper and consumed the largest effort and computational costs within this work. We therefore think it is a key contribution to the paper.

R#2: *Fig. 14: Explain what generates ‘surface wave fronts’ and how?*

AC: We think that the discussion about the generation of surface wave fronts is beyond the scope of this paper.

R#2: *Fig. 15: Why 5 lines, 4 legends?*

AC: In analogy to (Iverson 2010) we plot the standard deviation which is a grey line above and below the measured data